J|A|C|S
ARTICLES

Published on Web 12/14/2010

Hepatocyte Targeting and Intracellular Copper Chelation by a Thiol-Containing Glycocyclopeptide

Anaïs M. Pujol,[†] Martine Cuillel,[‡] Olivier Renaudet,[§] Colette Lebrun,[†] Peggy Charbonnier,[‡] Doris Cassio,[||] Christelle Gateau,[†] Pascal Dumy,[§] Elisabeth Mintz,[‡] and Pascale Delangle*,[†]

INAC, Service de Chimie Inorganique et Biologique (UMR_E 3 CEA UJF, FRE CNRS 3200), Commissariat à l'Energie Atomique, 17 Rue des Martyrs, 38054 Grenoble Cedex, France; iRTSV, Laboratoire de Chimie et Biologie des Métaux (UMR 5249 CEA CNRS UJF), Commissariat à l'Energie Atomique, 17 Rue des Martyrs, 38054 Grenoble Cedex, France; Département de Chimie Moléculaire (UMR 5250 CNRS UJF), Université Joseph Fourier, 38041 Grenoble cedex, France; and INSERM, UMR-S757, Université Paris-Sud, Orsay, 91405, France

Received July 13, 2010; E-mail: pascale.delangle@cea.fr.

Abstract: Metal overload plays an important role in several diseases or intoxications, like in Wilson's disease, a major genetic disorder of copper metabolism in humans. To efficiently and selectively decrease copper concentration in the liver that is highly damaged, chelators should be targeted at the hepatocytes. In the present work, we synthesized a molecule able to both lower intracellular copper, namely Cu(I), and target hepatocytes, combining within the same structure a chelating unit and a carbohydrate recognition element. A cyclodecapeptide scaffold displaying a controlled conformation with two independent faces was chosen to introduce both units. One face displays a cluster of carbohydrates to ensure an efficient recognition of the asialoglycoprotein receptors, expressed on the surface of hepatocytes. The second face is devoted to metal ion complexation thanks to the thiolate functions of two cysteine side-chains. To obtain a chelator that is active only once inside the cells, the two thiol functions were oxidized in a disulfide bridge to afford the glycopeptide $\mathbf{P}^3$. Two simple cyclodecapeptides modeling the reduced and complexing form of $\mathbf{P}^3$ in cells proved a high affinity for Cu(I) and a high selectivity with respect to Zn(II). As expected, $\mathbf{P}^3$ becomes an efficient Cu(I) chelator in the presence of glutathione that mimics the intracellular reducing environment. Finally, cellular uptake and ability to lower intracellular copper were demonstrated in hepatic cell lines, in particular in WIF-B9, making $\mathbf{P}^3$ a good candidate to fight copper overload in the liver.

1. Introduction

Metal overload plays an important role in several diseases or intoxications.[1] Among these metals, copper (Cu) is an essential element which is used as a cofactor in many redox proteins, involved in several vital processes. Free Cu can also promote Fenton-like reactions and would thus be very toxic even at low concentration. Therefore, intracellular Cu concentration needs to be rigorously controlled so that it is only provided to the essential enzymes but does not accumulate to toxic levels.[2] For instance, Wilson's disease is one of the major genetic disorder of Cu metabolism in humans. Impairment of the copper transport in hepatocytes, results in cytosolic Cu accumulation with associated cellular injury.[3,4] Cu is also involved in neurodegenerative diseases like Alzheimer's disease and suspected to cause Aβ precipitation and toxicity.[5,6] Therefore, as chelation therapy[1,4,5] is currently used or proposed for treating these disorders, it is of major interest to develop molecules able to efficiently and selectively bind Cu.

In particular, copper chelators are used to treat metal overload for patients suffering from copper homeostasis disorders like Wilson's disease.[7] In this disease, copper is accumulated in different parts of the patient's organism like the liver, the central nervous system, and the eyes.[8] Current treatments are aimed at lowering dietary copper uptake and not at fighting intracellular copper accumulation.[1,9] To efficiently and selectively decrease the copper concentration in the liver, an organ highly damaged in this disease, chelators should be targeted at the hepatocytes. In cells, excess copper is in the +I oxidation state.[3] In the present work, we designed a molecule able to both lower intracellular copper, namely Cu(I), and target hepatocytes, combining within

[†] INAC, Service de Chimie Inorganique et Biologique, Commissariat à l'Energie Atomique.
[‡] iRTSV, Laboratoire de Chimie et Biologie des Métaux, Commissariat à l'Energie Atomique.
[§] Département de Chimie Moléculaire, Université Joseph Fourier.
[||] INSERM, UMR-S757, Université Paris-Sud.

(1) Andersen, O. *Chem. Rev.* **1999**, *99*, 2683–2710.
(2) Rosenzweig, A. C. *Acc. Chem. Res.* **2001**, *34*, 119–128. Puig, S.; Thiele, D. J. *Curr. Opin. Chem. Biol.* **2002**, *6*, 171–180. Arnesano, F.; Banci, L.; Bertini, I.; Ciofi-Baffoni, S. *Eur. J. Inorg. Chem.* **2004**, 1583–1593.
(3) Tao, T. Y.; Gitlin, J. A. *Hepatology* **2003**, *37*, 1241–1247.
(4) Sarkar, B. *Chem. Rev.* **1999**, *99*, 2535–2544.
(5) Bush, A. I. *Trends Neurosci.* **2003**, *26*, 207–214.
(6) Gaggelli, E.; Kozlowski, H.; Valensin, D.; Valensin, G. *Chem. Rev.* **2006**, *106*, 1995–2044. Donnelly, P. S.; Xiao, Z. G.; Wedd, A. G. *Curr. Opin. Chem. Biol.* **2007**, *11*, 128–133. Faller, P.; Hureau, C. *Dalton Trans.* **2009**, 1080–1094.
(7) Das, S. K.; Ray, K. *Nat. Clin. Pract. Neuro.* **2006**, *2*, 482–493.
(8) Gitlin, J. D. *Gastroenterology* **2003**, *125*, 1868–1877.
(9) Brewer, G. J.; Askari, F. K. *J. Hepatol.* **2005**, *42*, S13–S21.

10.1021/ja106206z

Scheme 1. Sequence of the Model Peptide $\mathbf{P^C}$

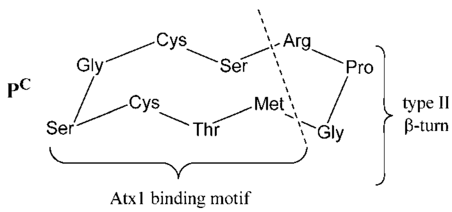

the same structure a chelating unit and a carbohydrate recognition element.

To design an efficient and selective copper chelating unit, we decided to take advantage of the high affinity of cysteine sulfur donors for Cu(I) evidenced in proteins trafficking or sequestering Cu in cells. As the cytoplasm of most cells is a reducing environment, the predominant oxidation state of Cu in cells is Cu(I). For instance, metallothioneins (MT) are small cysteine-rich proteins whose synthesis is induced when Cu is in excess of physiological requirements. They are sequestering Cu by forming Cu(I) clusters.[10] Many intracellular Cu transporters such as the yeast metallochaperone Atx1 contain the consensus MxCxxC sequence that binds soft metal ions with two cysteines.[11,12] A model peptide $\mathbf{P^C}$, incorporating the Atx1 binding sequence (MTCSGC, Scheme 1) was found highly selective for Cu(I) with respect to Zn(II), another essential metal ion found in cells.[13,14] In addition, we have also recently demonstrated that a tripodal pseudopeptide scaffold extended by three converging cysteines, mimics the selectivity of metallothioneins or other cysteine-rich proteins for the soft cations Cu(I) and Hg(II) with respect to other divalent ions.[15] Cysteine-based peptides or pseudopeptides appear to be efficient Cu(I) complexing molecules and we selected a peptide sequence with two cysteines to design the chelating unit.

A well-known strategy for targeting hepatocytes[16] is to use ligands of the asialoglycoprotein receptor (ASGP-R) which is uniquely expressed on the surface of these cells.[17] Indeed, ASGP-R is a human hepatic lectin, which recognizes terminal galactose (Gal) and *N*-acetylgalactosamine (GalNAc) with a higher affinity for GalNAc than for Gal.[18] The affinity of ligands for this receptor is strongly dependent on the valency and the display of sugar residues.[19] While the affinity between lectin and monosaccharides is weak ($K_D \approx 0.1-1$ mM), sugar-protein interactions can be greatly enhanced by multivalent events commonly known as the "cluster glycoside effect".[20] The efficiency of such targeting units has been demonstrated for gene or drug delivery to cultured cells or to animals.[21]

In the present work, we chose a decapeptide scaffold with two independent faces to form regioselectively addressable functionalized templates (RAFTs).[22] Such cyclodecapeptides incorporate two prolylglycine sequences as β-turn inducers to constrain the backbone conformation into an antiparallel β sheet.[23,24] They display a controlled conformation that has been exploited successfully for diverse applications such as the design of nanovectors, synthetic vaccines, and protein mimics.[22] In addition, we have demonstrated that clusters of carbohydrates grafted at the surface of the cyclodecapeptide scaffold ensure the specific recognition with a significantly enhanced affinity for lectins through multivalent interactions in solution[25] and on solid support.[26,27] Moreover, cyclodecapeptides displaying less than four sugars or unspecific sugar units clearly show negligible binding ability for the targeted lectins.[26,27] Therefore, four αGalNac units were chemioselectively grafted on the upper face of this cyclodecapeptide which is then devoted to ASGP-R recognition and targeting. It has been estimated by molecular modeling that the distance between two sugar units is in the 15−25 Å range, which is similar to the distance between two binding sites in ASGP-R.[18,19] We thus expect that our vector binds to the ASGP-R through an efficient intramolecular mechanism (chelate effect).[28,29] Another advantage of such cyclopeptide scaffolds is the spatial separation between targeting and "drug-delivery" domains.[22,30] The lower face was used for soft metal ion complexation thanks to the thiol functions of two cysteines in the cyclopeptide sequence (Scheme 2). These thiol functions have been oxidized in a disulfide bridge to afford $\mathbf{P}^3$, which is stable in the presence of oxygen and most importantly which is not an efficient chelator before entering the hepatic cells: therefore, $\mathbf{P}^3$ can be considered as a prodrug activated in the reductive medium of the targeted cells (Scheme 2). Finally, one glycine among the β-turns, has been replaced by a D-lysine to introduce an organic fluorophore (TRITC) and to visualize the uptake of the compound in hepatic cell lines.

In this work, to assess the metal complexation properties of the reduced and active form of the targeting chelator $\mathbf{P}^3$ in cells, we first investigated two simple cyclodecapeptides devoid of the targeting units. These model peptides bear two cysteines in positions 2 and 7 mimicking the complexing unit of $\mathbf{P}^3$ in cells. As these cyclodecapeptides proved a high affinity for Cu(I) as well as a high selectivity with respect to Zn(II), the cyclopeptides bearing the targeting sugar units $\mathbf{P}^3$ and $\mathbf{P^3}$-TRITC represented

(10) Koch, K. A.; Pena, M. M. O.; Thiele, D. J. *Chem. Biol.* **1997**, *4*, 549–560. Stillman, M. J. *Coord. Chem. Rev.* **1995**, *144*, 461–511.
(11) Rosenzweig, A. C.; O'Halloran, T. V. *Curr. Opin. Chem. Biol.* **2000**, *4*, 140–147. Arnesano, F.; Banci, L.; Bertini, I.; Ciofi-Baffoni, S.; Molteni, E.; Huffman, D. L.; O'Halloran, T. V. *Genome Res.* **2002**, *12*, 255–271.
(12) Opella, S. J.; DeSilva, T. M.; Veglia, G. *Curr. Opin. Struct. Biol.* **2002**, *6*, 217–223.
(13) Rousselot-Pailley, P.; Sénèque, O.; Lebrun, C.; Crouzy, S.; Boturyn, D.; Dumy, P.; Ferrand, M.; Delangle, P. *Inorg. Chem.* **2006**, *45*, 5510–5520.
(14) Sénèque, O.; Crouzy, S.; Boturyn, D.; Dumy, P.; Ferrand, M.; Delangle, P. *Chem. Commun.* **2004**, 770–771.
(15) Pujol, A. M.; Gateau, C.; Lebrun, C.; Delangle, P. *J. Am. Chem. Soc.* **2009**, *131*, 6928–6929.
(16) Wu, J.; Nantz, M. H.; Zern, M. A. *Front. Biosci.* **2002**, *7*, d717–725.
(17) Ashwell, G.; Harford, J. *Annu. Rev. Biochem.* **1982**, *51*, 531–554. Spiess, M. *Biochemistry* **1990**, *29*, 10009–10018.
(18) Baenziger, J. U.; Maynard, Y. *J. Biol. Chem.* **1980**, *255*, 4607–4613.
(19) Lee, Y. C.; Townsend, R. R.; Hardy, M. R.; Lonngren, J.; Arnarp, J.; Haraldsson, M.; Lonn, H. *J. Biol. Chem.* **1983**, *258*, 199–202.
(20) Lee, Y. C.; Lee, R. T. *Acc. Chem. Res.* **1995**, *28*, 321–327.
(21) Kim, E. M.; Jeong, H. J.; Park, I. K.; Cho, C. S.; Moon, H. B.; Yu, D. Y.; Bom, H. S.; Sohn, M. H.; Oh, I. J. *J. Controlled Release* **2005**, *108*, 557–567. Cai, G.; Jiang, M.; Zhang, B.; Zhou, Y.; Zhang, L.; Lei, J.; Gu, X.; Cao, G.; Jin, J.; Zhang, R. *Biol. Pharm. Bull.* **2009**, *32*, 440–443. Yang, W.; Mou, T.; Peng, C.; Wu, Z.; Zhang, X.; Li, F.; Ma, Y. *Bioorg. Med. Chem.* **2009**, *17*, 7510–7516.
(22) Boturyn, D.; Defrancq, E.; Dolphin, G. T.; Garcia, J.; Labbe, P.; Renaudet, O.; Dumy, P. *J. Pept. Sci.* **2008**, *14*, 224–240.
(23) Dumy, P.; Eggleston, I. M.; Esposito, G.; Nicula, S.; Mutter, M. *Biopolymers* **1996**, *39*, 297–308.
(24) Peluso, S.; Rückle, T.; Lehmann, C.; Mutter, M.; Peggion, C.; Crisma, M. *ChemBioChem* **2001**, *2*, 432–437. Bonnet, C. S.; Fries, P. H.; Crouzy, S.; Sénèque, O.; Cisnetti, F.; Boturyn, D.; Dumy, P.; Delangle, P. *Chem. Eur. J.* **2009**, *15*, 7083–7093.
(25) Renaudet, O.; Dumy, P. *Org. Lett.* **2003**, *5*, 243–246.
(26) Singh, Y.; Renaudet, O.; Defrancq, E.; Dumy, P. *Org. Lett.* **2005**, *7*, 1359–1362.
(27) Renaudet, O.; Dumy, P. *Org. Biomol. Chem.* **2006**, *4*, 2628–2636.
(28) Lundquist, J. J.; Toone, E. J. *Chem. Rev.* **2002**, *102*, 555–578.
(29) Wilczewski, M.; Van der Heyden, A.; Renaudet, O.; Dumy, P.; Coche-Guerente, L.; Labbe, P. *Org. Biomol. Chem.* **2008**, *6*, 1114–1122.
(30) Renaudet, O. *Mini-Rev. Org. Chem.* **2008**, *5*, 274–286.

Scheme 2. General Structure of Cu(I) Chelators Designed to Target Hepatocytes

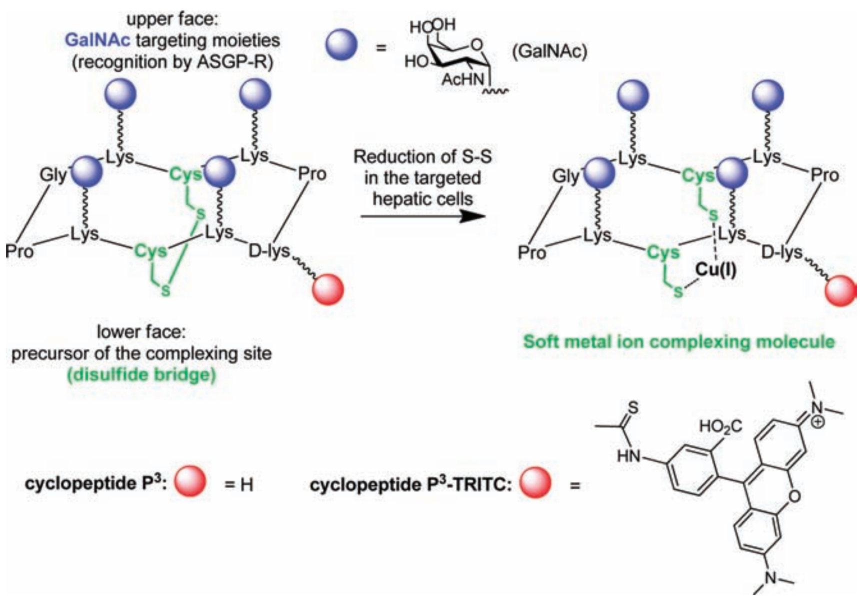

Scheme 3. Formula of the Cyclodecapeptides $\mathbf{P}^1$ and $\mathbf{P}^2$ Which Bear Two Coordinating Cysteines in Positions 2 and 7[a]

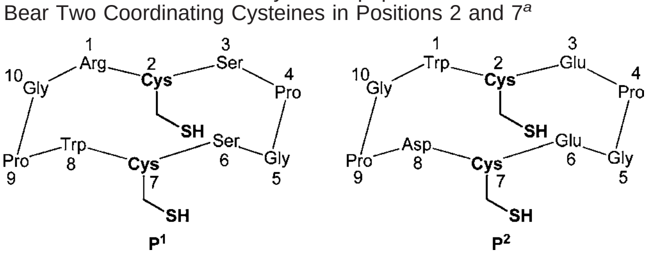

[a] Only the side-chains of cysteines have been represented.

in Scheme 2 were next synthesized. In vitro complexation studies with $\mathbf{P}^3$ demonstrated that this molecule binds Cu(I) only in a reducing medium, mimicking the intracellular compartment. Finally, cellular uptake and ability to lower intracellular copper were demonstrated in hepatic cell lines, making $\mathbf{P}^3$ a good candidate to fight copper overload in the liver.

2. Results and Discussion

2.1. Synthesis and Characterization of the Model Chelating Peptides $\mathbf{P}^1$ and $\mathbf{P}^2$. The two cyclodecapeptides $\mathbf{P}^1$ and $\mathbf{P}^2$ (Scheme 3) bearing two cysteines in positions 2 and 7 and modeling the reduced and active form of the targeting chelator $\mathbf{P}^3$ in cells were first synthesized to evaluate their complexing ability for Cu(I) and divalent metal ions. A tryptophane residue was inserted in position 1 or 8 of the two model peptides to determine precisely the peptide concentration by measuring the absorbance of the indole moiety at 280 nm. In $\mathbf{P}^1$, three polar residues (2 serines and one arginine) mimic the hydrophilicity of the sugar moieties on the upper face of $\mathbf{P}^3$. Aspartic and glutamic acids were inserted in the sequence of $\mathbf{P}^2$ to provide a second model peptide with a negatively charged upper face bearing three carboxylate groups at physiological pH. This less realistic model of $\mathbf{P}^3$ was designed to evaluate the influence of the upper face on the complexation properties of the two cysteines side-chains located at the lower face.

Classical solid-phase synthesis using Fmoc strategy was used to synthesize $\mathbf{P}^1$ and $\mathbf{P}^2$. The 10-mer-protected precursors were assembled on the resin and cyclized in dichloromethane after cleavage from the resin. The side chains were subsequently deprotected. $\mathbf{P}^1$ and $\mathbf{P}^2$ are sensitive to air oxidation and were therefore stored and manipulated under argon in a glovebox.

Several isomers were detected in the NMR spectra of the two peptides, the major one representing ~70% of the total peptide concentration at 298 K. The evolution of the proportions of the different species as a function of temperature confirms that the latter are conformers in equilibrium at the NMR time scale. The two major species were fully assigned from a combination of COSY, TOCSY, and ROESY spectra following standard assignment procedures (see Tables S1 and S2 in the Supporting Information).[31]

In the major conformers of the two peptides, the trans conformation of the peptide bonds with prolines are evidenced by the presence of the short contacts (X3 Hα, Pro4 Hδ) and (X8 Hα, Pro9 Hδ). The XPGX motifs show the characteristic features of type II β-turn structures:[32] a cis relationship between Gly5 NH and Pro4 Hα (2.2 Å) and between Gly10 NH and Pro9 Hα (2.2 Å). Strong ROE cross peaks are also detected between X6 NH and Pro4 Hα (3.3 Å) or X1 NH and Pro10 Hα (3.3−3.5 Å). Finally, a short contact is detected between X6 NH and Gly5 NH or X1 NH and Gly10 NH (2.8−2.9 Å). These distances are reported in Table S4 of the Supporting Information.

The resonances of the minor conformers are not very intense which prevents their full characterization. As proposed by several authors,[23,33] they may correspond to isomerization of X-Pro bonds into cis isomer. Nevertheless, the two compounds $\mathbf{P}^1$ and $\mathbf{P}^2$ are good models of cyclodecapeptides bearing two cysteines in position 2 and 7 to coordinate soft metal ions.

2.2. Copper(I) Binding by the Model Peptides $\mathbf{P}^1$ and $\mathbf{P}^2$. Binding of Cu(I) with the two model peptides $\mathbf{P}^1$ and $\mathbf{P}^1$ was investigated by UV and CD spectroscopy. It is known that Cu(I) disproportionates in Cu(0) and Cu(II) in water. Therefore, the experiments with this cation were conducted in the presence of acetonitrile which associates with Cu(I) and overcomes the

(31) Wüthrich, K. *NMR of Proteins and Nucleic Acids*; Wiley: New York, 1986.
(32) Wüthrich, K.; Billeter, M.; Braun, W. *J. Mol. Biol.* **1984**, *180*, 715–740.
(33) Peng, Z.-H. *Biopolymers* **1999**, *49*, 565–574.

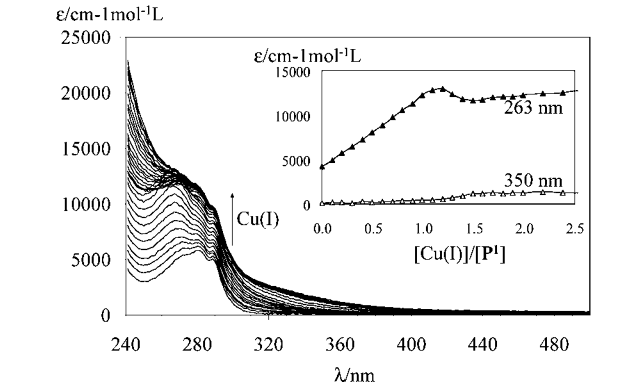

Figure 1. UV titration of **P**[1] (65 μM) with Cu(I) at pH 7.4 (20 mM phosphate buffer/CH_3CN ($v/v = 9/1$)) at 298 K.

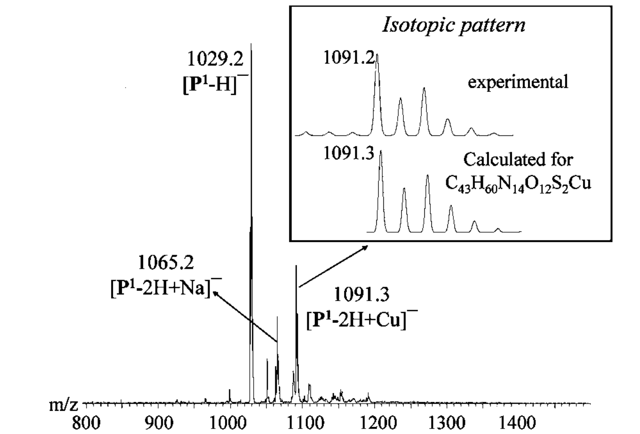

Figure 2. (−) ESI mass spectrum of a solution containing **P**[1] (50 μM) and 1.0 equiv Cu(I) in $AcONH_4$ buffer (20 mM, pH 7).

disproportionation reaction.[34] Binding of Cu(I) to the peptides was first monitored by UV spectroscopy. The addition of aliquots of tetrakis(acetonitrile) copper(I) hexafluorophosphate dissolved in acetonitrile over a peptide solution in a 9/1 (v/v) mixture of phosphate buffer (20 mM, pH 7.4) and acetonitrile results in the appearance of a band centered at 263 nm that linearly increases with increasing Cu(I) concentration up to 1 equiv. This band is characteristic of charge-transfer transitions (LMCT) of the thiolate−Cu(I) bonds.[35] The extinction coefficient of this LMCT bands are 7620 and 7640 $M^{-1}cm^{-1}$ for Cu**P**[1] and Cu**P**[2] complexes, respectively. These values are compatible with the value found in MT of ~7000/Cu bound.[36] In excess of Cu(I) other transitions appear, in particular at lower energy (350 nm), which may be attributed to the formation of often-encountered Cu(I)-thiolate clusters.[35,37] Typical absorption spectra of Cu(I) into a solution of **P**[1] at pH 7.4 are illustrated in Figure 1.

The formation of a unique complex from 0 to 1 Cu equiv was confirmed by CD titrations. Indeed, intense dichroic bands develop in the CD spectrum of Cu**P**[1] with positive and negative maxima at (+) 263 nm and (−) 289 nm that are attributed to thiolate−Cu LMCT transitions.[36] An isodichroic point is detected at 279 nm from 0 to 1 Cu(I) equiv demonstrating that the free peptide is transformed in only one complex.

These data are similar to what we observed with **P**[C] (Scheme 1), the model peptide of the yeast copper chaperone binding loop.[13] In this case, the monomolecular nature of the Cu**P** complexes could be demonstrated by investigating diffusion coefficients by Pulse Field Gradient NMR, and relating them to the volume of the species. Unfortunately, the copper complexes of **P**[1] and **P**[2] were too insoluble in the concentration range of ^{1}H NMR (1 mM) to allow us to obtain reliable diffusion data for them. Nevertheless, the mononuclear complex Cu**P**[1] (1091.25, [**P**[1]+Cu-2H]$^-$) is nicely evidenced in the (−)ESI-MS spectra, as illustrated in Figure 2. In excess of Cu(I), higher nuclearity complexes are detected like [**P**[1]+2Cu-3H]$^-$ at 1155.17 and [2**P**[1]+4Cu-2H]$^{2+}$ at 1157.2. The same tendency is observed with **P**[2] even though the ESI-MS spectra are complicated by the formation of many sodium and potassium adducts due to the presence of three carboxylate functions in the free ligand.

To determine the conditional stability constants of the two Cu(I) peptide complexes (Cu**P**) at physiological pH, UV−visible titrations were performed in presence of a chelator of known affinity. Bathocuproine disulfonate (Na_2BCS) has been demonstrated to form a stable 1:2 complex, $Cu(BCS)_2^{3-}$, according to eq 1 with a constant, $\log\beta_{12} = 19.8$.[37]

$$Cu^+ + 2\,BCS^{2-} = Cu(BCS)_2^{3-} \qquad (1)$$

The complex $Cu(BCS)_2^{3-}$ exhibits an absorption band in the visible region with its maximum at 483 nm ($\epsilon = 13300$ $M^{-1}cm^{-1}$). Titrations of the peptides **P**[1] and **P**[2] preloaded with 0.8−0.9 equiv of Cu(I), with aliquots of the competitor (BCS^{2-}) solution shows the appearance of the absorption band of $Cu(BCS)_2^{3-}$ that corresponds to the transfer of the metal cation from the peptide to BCS^{2-}. These spectroscopic data were fitted according to eq 2 with the following conditional affinity constants: $\log\beta_{11}(\mathbf{P}^1) = 16.7(1)$ and $\log\beta_{11}(\mathbf{P}^2) = 15.5(1)$.

$$Cu\mathbf{P} + 2\,BCS^{2-} = \mathbf{P} + Cu(BCS)_2^{3-} \qquad (2)$$

It appears clearly that **P**[2] is a less efficient copper complexing agent than **P**[1] (or **P**[C]). This difference can be attributed to the presence of the three negatively charged carboxylate functions which induce a charge repulsion with the CuS_2^- copper center. Unlike **P**[2], **P**[1] bears three neutral amino acids (1 Trp and 2 Ser) and a positively charged amino acid (Arg). The values of the affinity constants determined for the copper complexes of **P**[1] and **P**[2] are somewhat lower than those reported for the model peptide of Atx1 (17.4 at pH 7.4)[13,14] or for the whole Atx1 protein.[37,38]

2.3. Divalent Metal Ion Complexes of P[1] and P[2]. Peptide sequences with two cysteines are known to efficiently complex soft or borderline divalent metal ions like Hg(II), Cd(II), Pb(II), and Zn(II).[12,39] In particular, the affinity for Zn(II) which is a potential competitor of Cu(I) in cells is an important parameter. Therefore, the complexes of the two model peptides **P**[1] and **P**[2]

(34) Kamau, P.; Jordan, R. B. *Inorg. Chem.* **2001**, *40*, 3879–3883.
(35) Fujisawa, K.; Imai, S.; Kitajima, N.; Moro-oka, Y. *Inorg. Chem.* **1998**, *37*, 168–169.
(36) Pountney, D. L.; Schauwecker, I.; Zarn, J.; Vasak, M. *Biochemistry* **1994**, *33*, 9699–9705. Faller, P.; Vasak, M. *Biochemistry* **1997**, *36*, 13341–13348.
(37) Xiao, Z.; Loughlin, F.; George, G. N.; Howlett, G. J.; Wedd, A. G. *J. Am. Chem. Soc.* **2004**, *126*, 3081–3090.
(38) Miras, R.; Morin, I.; Jacquin, O.; Cuillel, M.; Guillain, F.; Mintz, E. *J. Biol. Inorg. Chem.* **2008**, *13*, 195–205.
(39) Rossy, E.; Seneque, O.; Lascoux, D.; Lemaire, D.; Crouzy, S.; Delangle, P.; Coves, J. *FEBS Lett.* **2004**, *575*, 86–90. Pufahl, R. A.; Singer, C. P.; Peariso, K. L.; Lin, S.-J.; Schmidt, P. J.; Fahrni, C. J.; Culotta, V. C.; Penner-Hahn, J. E.; O'Halloran, T. V. *Science* **1997**, *278*, 853–856. DiDonato, M.; Zhang, J.; Que, L, Jr.; Sarkar, B. *J. Biol. Chem.* **2002**, *277*, 13409–13414. Banci, L.; Bertini, I.; Ciofi-Baffoni, S.; Su, X. C.; Miras, R.; Bal, N.; Mintz, E.; Catty, P.; Shokes, J. E.; Scott, R. A. *J. Mol. Biol.* **2006**, *356*, 638–650.

Table 1. LMCT Band Characteristics for Hg(II), Cd(II), Pb(II), and Cu(I) Complexes with **P**[1] and **P**[2], with $\Delta\epsilon = \epsilon(\mathrm{MP}) - \epsilon(\mathrm{P})$

	P^1		P^2	
	λ (nm)	$\Delta\epsilon$ ($M^{-1}cm^{-1}$)	λ (nm)	$\Delta\epsilon$ ($M^{-1}cm^{-1}$)
Hg**P**[a]	210	13 600	210	18 600
	250	870	250	1 500
Cd**P**[a]			220	10 000
Cd(**P**)$_2$[a]	230	21 000		
Pb**P**[b]	320	3 000	310	3500
Pb(**P**)$_2$[b]	338	4 000		
Cu(**P**)[a]	263	7 620	263	7 640

[a] Phosphate buffer 20 mM, pH 7.4. [b] Bis-Tris buffer 20 mM, pH 7.

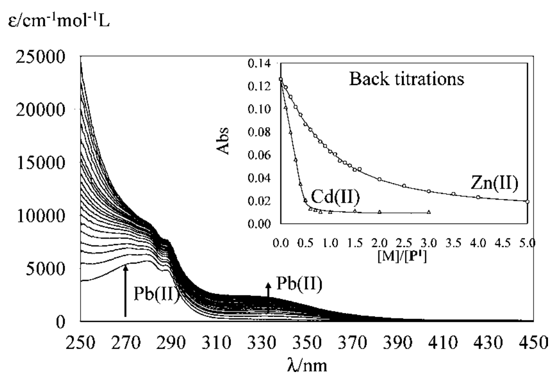

Figure 3. UV titration of **P**[1] (65 μM) with lead chloride at pH 7.0 (20 mM Bis-Tris). Spectra correspond to samples with 0−5 equiv of Pb(II) per **P**[1]. Inset: absorbances at 330 nm during the back-titrations of Pb**P**[1] ([**P**[1]] = 55 μM; [Pb] = 165 μM) with $CdCl_2$ (triangles) and $ZnCl_2$ (circles). The calculated lines were generated in specfit.

with divalent metal ions were also investigated by ESI-MS and UV spectroscopy. The UV titrations show the expected LMCT bands,[40,41] whose characteristics are reported in Table 1. Figure 3 illustrates the typical absorption spectra for the titration of Pb(II) into a solution of **P**[1] at pH 7. Two successive complexes are detected in this titration as observed earlier with $\mathbf{P^C}$,[13] whereas only the ML complex is detected in a similar titration with **P**[2]. The ESI-MS spectra show systematically the presence of the unique ML complex with **P**[2] whereas both species ML and ML_2 are seen with **P**[1] (Table S5 of the Supporting Information). The stability constants have been measured as previously described with model peptides of the yeast copper chaperone Atx1, in Bis-Tris buffer, by analyzing the direct titration of the peptide with Pb(II) and the competition titration starting from the lead complex for Cd(II) and Zn(II).[13,40] For instance, it can be seen in the inset of Figure 3 that only 0.5 equiv of Cd(II) are needed to displace Pb(II) from the complex Pb**P**[1], confirming the formation of the species Cd($\mathbf{P}^1$)$_2$ species.

Data collected in Table 2 show rather similar results to those obtained previously with the peptide $\mathbf{P^C}$, which mimics Atx1 binding loop.[13,14] The selectivity, Hg(II) > Cu(I) ≫ Cd(II) ≈ Pb(II) > Zn(II) is common for thiol-rich ligands. The metal complexes of **P**[1] and **P**[2] are systematically less stable than those of $\mathbf{P^C}$, indicating that the more rigid cyclodecapeptide scaffold of **P**[1] and **P**[2] with two cysteines in positions 2 and 7 has a lower affinity for metal ions than the flexible binding loop of $\mathbf{P^C}$, which can easily adapt to different coordination geometry.[14] Perhaps the most striking feature is that **P**[1] tends to form ML_2 complexes,

Table 2. Apparent Equilibrium Constants (logβ_{pq}) at pH 7 and 298 K, in 20 mM Bis-Tris, $\beta_{pq} = [M_pP_q]/[M]^p[P]^q$

M	logβ_{pq}	P^1	P^2	P^C
Pb(II)	logβ_{11}	7.4(2)	7.1(1)	8.0(1)
	logβ_{12}	11.9(5)		12.5(7)
Cd(II)	logβ_{11}		7.0(1)	9.2(1)
	logβ_{12}	15.0(2)		15.6(1)
Zn(II)	logβ_{11}	6.6(1)	5.9(1)	6.8(2)
Hg(II)	logβ_{11}	>19.7[a]	>18.5[a]	>18.6
Cu(I)	logβ_{11}	16.7(1)[a]	15.5(1)[a]	16.6(1)

[a] At pH 7.4 in 20 mM phosphate buffer.

whether **P**[2] forms only ML complexes. These two observations could be the result of the negative charge (3^-) of the "upper" face of the cyclodecapeptide **P**[2] due to the three carboxylate functions, which may induce electrostatic repulsions in the metal complexes and in particular in the species M($\mathbf{P}^2$)$_2$. Moreover, **P**[2] has a lower affinity than **P**[1].

These experiments have clearly demonstrated that the two cyclodecapeptides **P**[1] and **P**[2] bearing two cysteines oriented on one face of the scaffold are efficient binders of soft ions Cu(I) and Hg(II) with a high selectivity with respect to Zn(II), an essential metal ion for the cell. This design allowed us to use the second face of the peptide scaffold to introduce ligands of the ASGP-R to target the Cu(I) complexing peptides at the hepatocytes. **P**[3], the resulting molecule, is expected to enter hepatocytes and once in the cells to bind Cu(I) without perturbing Zn(II) homeostasis. **P**[3] should also be an efficient chelator of intracellular Hg(II) if the cells were exposed to mercury.

2.4. Synthesis of the Targeted Peptides P[3] and P[3]-TRITC. The syntheses of **P**[3] and **P**[3]-TRITC are described in Scheme 4. Classical solid-phase peptide synthesis using the Fmoc strategy was used to assemble the linear intermediate **1** on a 2-chlorotrityl chloride resin, starting from commercial Fmoc protected amino acids and the Fmoc-Lys[Boc-Ser(*t*Bu)]−OH building block, which was obtained from Boc-Ser(*t*Bu)−OSu and Fmoc-Lys-OH as previously described.[42] The on-resin linear peptide **1** was then oxidized with iodine to afford the disulfide compound **2**, which was then cleaved from the resin in mild acidic conditions and subsequently cyclized in DMF to afford the protected cyclodecapeptide **3**. After deprotection of the lysine side-chains by acidolysis, **4** was obtained with a 33% overall yield from **1**.

The incorporation of carbohydrate recognition motifs was performed following an oxime-based strategy from the aminooxylated sugars.[27] Although sodium periodate is known to oxidize thioethers[43] and disulfide bridges,[44] the selective oxidation of serines in the presence of disulfide bridges has recently been described.[45] Following this procedure, we have treated **4** with sodium periodate to afford the cyclodecapeptide **5** which presents four glyoxyaldehyde functions with a 15% yield. However, the thiosulfinate byproduct was evidenced by mass spectrometry (M(**4**) + 16) and isolated in nearly 40%, even working with stoichiometric amounts of sodium periodate (4 equiv.) and short reaction times (15 min). Then the oxime conjugation of **5** with an excess of O-α-D-*N*-acetylgalactopyranosyl oxyamine (αGalNAcONH_2, **6**),[27] afforded the desired compound **P**[3]. Finally, tetramethylrhodamine isothiocyanate

(40) Payne, J. C.; terHorst, M. A.; Godwin, H. A. *J. Am. Chem. Soc.* **1999**, *121*, 6850–6855.
(41) Matzapetakis, M.; Farrer, B. T.; Weng, T.-C.; Hemmingsen, L.; Penner-Hahn, J. E.; Pecoraro, V. L. *J. Am. Chem. Soc.* **2002**, *124*, 8042–8054.
(42) Fouillard, S.; Rasmussen, M. O.; Razkin, J.; Boturyn, D.; Dumy, P. *J. Org. Chem.* **2008**, *73*, 983–991.
(43) Hiskey, R. G.; Harpold, M. A. *J. Org. Chem.* **1967**, *32*, 3191–3194.
(44) Juaristi, E.; Cruz-Sanchez, J. S. *J. Org. Chem.* **1988**, *53*, 3334–3338.
(45) Avrutina, O.; Schmoldt, H. U.; Gabrijelcic-Geiger, D.; Wentzel, A.; Frauendorf, H.; Sommerhoff, C. P.; Diederichsen, U.; Kolmar, H. *ChemBioChem* **2008**, *9*, 33–37.

Scheme 4. Syntheses of the Derivatives **P**^{3} and **P^3**-TRITC[a]

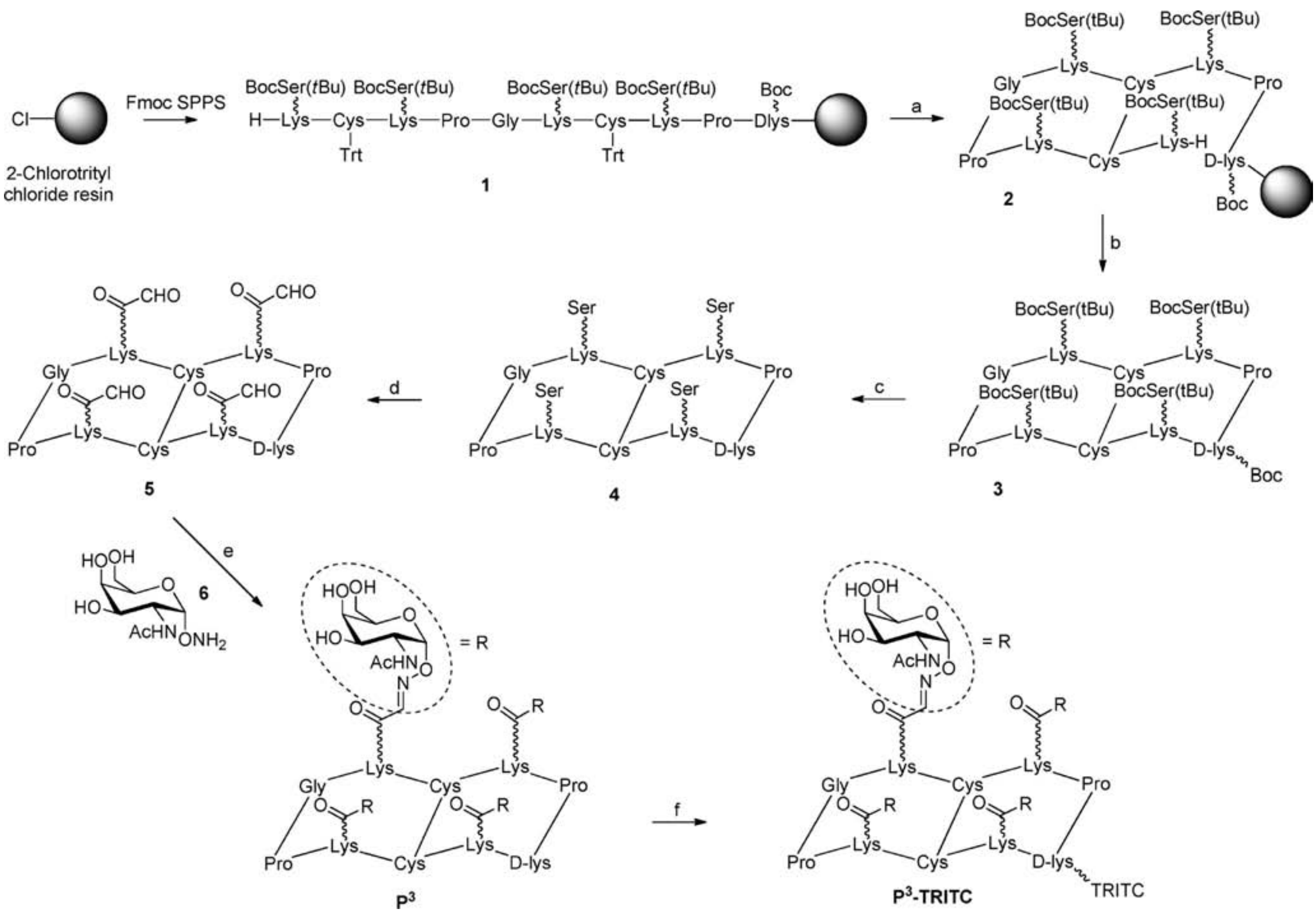

[a] Reagents and conditions: (a) I_2, DMF; (b) i: TFA/CH_2Cl_2 1%; ii; PyBOP, DIEA, DMF; (c) TFA/TIS/H_2O (95:2.5:2.5); (d) $NaIO_4$, H_2O; (e) **6**, 10% AcOH aq.; and (f) TRITC, DIEA, DMF.

(TRITC) was coupled to the D-Lys side chain of **P**^{3} to give the red-fluorescent compound **P^3**-TRITC.

2.5. Copper Complexation by P^3. The ability of **P**^{3} to complex copper was evaluated using BCS as a Cu(I) chelator as described in Section 2.2. Indeed, the absorption of the orange complex $Cu(BCS)_2{}^{3-}$ gives the amount of copper bound to BCS and therefore, the more intense is this band, the lower is the affinity of the peptide for Cu(I).

As expected, **P**^{3} does not bind to Cu(I) as it contains a disulfide bridge and no free thiolate functions: as seen in Figure 4, in that case 100% of Cu is bound to BCS. To mimic the reducing intracellular medium, 1 mM of glutathione (GSH) was introduced into the sample.[46] This induced a decrease of the $Cu(BCS)_2$ complex absorption to 40% of the total Cu, which can be interpreted by the reduction of the disulfide bridge of **P**^{3} by GSH to afford $\mathbf{P}^3_{SH\text{-}SH}$ that contains two thiolate functions and is therefore able to complex Cu(I). Interestingly, as seen in Figure 4, $\mathbf{P}^3_{SH\text{-}SH}$ binds Cu(I) with an affinity which is between those measured with the two peptides **P**^{1} and **P**^{2} mimicking $\mathbf{P}^3_{SH\text{-}SH}$ binding site. As GSH is known to complex Cu(I),[47] copper uptake by 1 mM GSH in the absence of peptide was evaluated.

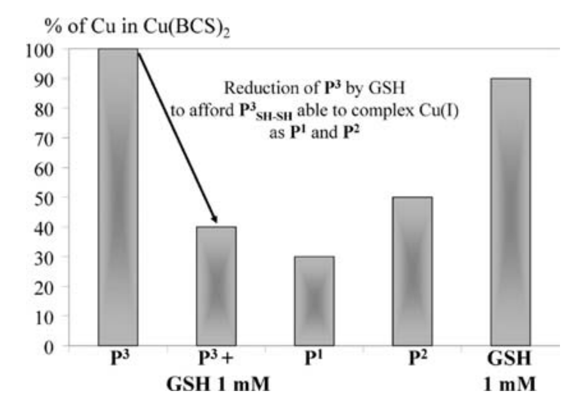

Figure 4. Percentage of Cu in the complex $Cu(BCS)_2$ for samples containing [Cu] = 0.9[**P**], [**P**] = 50 μM, and [BCS] = 2[Cu] in 20 mM phosphate buffer, pH 7.4 at 298 K.

This induced a decrease of the $Cu(BCS)_2$ complex absorption to only 90% of the total Cu, therefore insignificant in comparison with the effect of reduced **P**^{3}.

These experiments demonstrate that **P**^{3} is not a copper complexing agent. However, once reduced by GSH, **P**^{3} becomes an efficient Cu(I) chelator. A similar activation of **P**^{3} is therefore expected to occur in the cells.

2.6. P^3 and P^3-TRITC in Hepatic Cell Lines. Hepatocytes are polarized cells, displaying apical poles in contact with the outer medium, basal poles in contact with the inner medium, and lateral poles in contact with adjacent cells. In the liver, the outer

(46) Meister, A.; Anderson, M. E. *Annu. Rev. Biochem.* **1983**, *52*, 711–760.

(47) Österberg, R.; Ligaarden, R.; Persson, D. *J. Inorg. Biochem.* **1979**, *10*, 341–355. Corazza, A.; Harvey, I.; Sadler, P. J. *Eur. J. Biochem.* **1996**, *236*, 697–705. Poger, D.; Fillaux, C.; Miras, R.; Crouzy, S.; Delangle, P.; Mintz, E.; Den Auwer, C.; Ferrand, M. *J. Biol. Inorg. Chem.* **2008**, *13*, 1239–1248.

medium is represented by a complex net of bile canaliculi formed by the union of apical poles of adjacent hepatocytes, sealed by tight junctions, and in which bile is collected. The inner medium is blood. ASGP-R is embedded in the basal (also called sinusoidal) membrane. Transport of molecules across the cell is an typical characteristic of hepatocytes. It is performed by a number of carrier proteins localized either at the sinusoidal or at the canalicular membrane. Unfortunately, this uneven distribution which ensures vectorial transport across hepatocytes is not easy to maintain in primary cultures (the bile acid uptake toward canaliculus decreases and disappears in 1−4 days).[48]

To study the ability of our chelators to bind Cu(I) inside cells, we used different hepatic cell lines. We first checked that **P**^{3}-TRITC would enter HepG2 cells, the most commonly used human hepatic cell line. Since HepG2 cells are poorly polarized, we also followed the chelator entry in WIF-B9 cells, which are able to reconstitute remarkably stable and polarized epithelia with functional bile canaliculi within 7−10 days.[49]

As recalled in the introduction, cells cannot cope with excesses of copper. When hepatocytes are subjected to high copper concentrations in the outer medium such as 20−200 μM, their first reaction is to pump copper out of the intracellular medium. To achieve this, ATP7B, their copper pump is recruited by moving toward the canalicular membrane to transfer copper into the bile. Although copper-induced ATP7B trafficking has been observed in both HepG2 and WIF-B9 cells,[50,51] the latter were preferred for their well-defined canalicular membrane. Indeed, WIF-B9 cells allowed us to use ATP7B intracellular localization changes to witness changes in the intracellular copper concentration.[51]

2.6.1. Entry of P^3-TRITC in Hepatic Cell Lines. The cells were kept in culture for the time needed to reconstitute an epithelium. For comparison, we have observed the kinetics of **P**^{3}-TRITC uptake by HepG2 and WIF-B9 cells. The molecule was visualized inside the cells by the red fluorescence signal of tetramethylrhodamine. As shown in Figure 5, HepG2 cells in contact with 0.2 μM **P**^{3}-TRITC for 2 h have incorporated some of the fluorescence dye. The longer the incubation, the more dye was incorporated, suggesting that the cells were progressively loaded with **P**^{3}-TRITC, although the presence of non-fluorescent cells was noticed even after 24 h of incubation, as expected from their low expression of ASPG-R.[52] A stronger fluorescent signal was observed in WIF-B9 cells after 2 h of incubation. This signal increased with time and after 24 h, all cells have accumulated **P**^{1}-TRITC. Moreover, the dye was concentrated around the bile canaliculi and fluorescence was detected in some canalicular spaces. Therefore, the **P**^{3}-TRITC molecule is able to get inside the cells within 2 h, to accumulate, and even to reach the bile canaliculus within a few hours.

2.6.2. Copper Complexation in Hepatic Cells. In the present study, we used the trafficking of ATP7B as a sensor of intracellular copper concentration changes. ATP7B belongs to

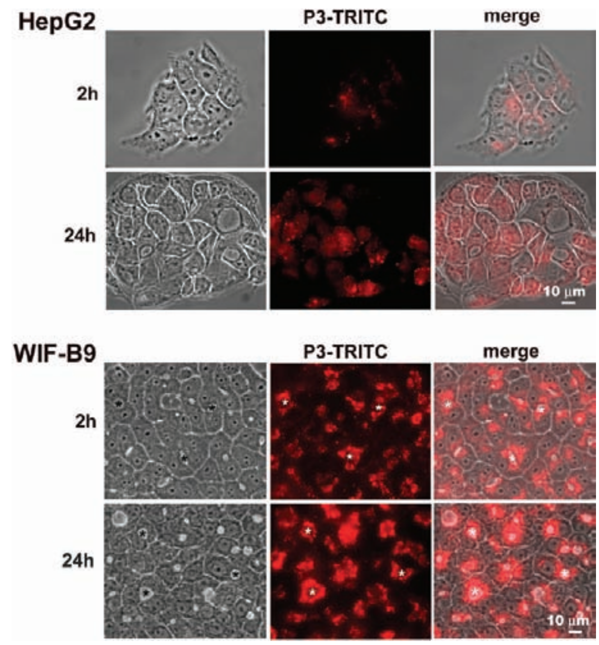

Figure 5. **P**^{3}-TRITC (0.2 μM) uptake by HepG2 and WIF-B9 cells. In the phase contrast image (left panels), the light gray spaces between adjacent WIF-B9 cells correspond to bile canaliculi, some of which are indicated by an asterisk.

the P-type ATPase family of cation-transporting membrane proteins which use ATP hydrolysis to transport ions across the membrane against their electrochemical gradient. ATP7B changes its localization in response to changes in intracellular Cu: under low-Cu conditions ATP7B plays its housekeeping role in the trans-Golgi network, close to the nucleus; under high-Cu conditions, ATP7B plays its detoxification role in the membrane of small cytoplasmic vesicles close to the canalicular membrane.[3] These vesicles are thought to be filled with Cu that is eventually thrown out of the cell into the canaliculus. Therefore, thanks to the well-defined canalicular membrane of WIF-B9 cells, ATP7B localization can be seen as an indicator of intracellular copper.

First of all, we determined the lowest copper concentration that would induce a clear trafficking of the endogenous ATP7B. A typical example is shown in Figure 6, where ATP7B (in green) was localized in cells incubated with the basal copper concentration found in the culture medium (Cu $\approx$ 0.01 μM) and in cells incubated for 2 h in the culture medium supplemented with 1 μM Cu. In low-Cu, ATP7B is present in the trans-Golgi network near the nucleus; in high-Cu, ATP7B is mainly localized in a continuous crown around the canaliculus to excrete the excess of copper, as expected.[51] This experiment demonstrates that the localization of ATP7B is a sensor of intracellular copper and can therefore be used to assess the ability of **P**^{3} to lower intracellular copper.

Therefore, the next step was to test the effect of **P**^{3} on ATP7B intracellular localization. To achieve this, WIF-B9 cells were incubated with 1 μM Cu for 2 h, followed by the addition of 10 μM **P**^{3} to the culture medium for 3 h (Figure 7B), or no chelator for control (Figure 7A). In these experiments, ATP7B (in green) was localized together with ZO-1 (in red), a protein which belongs to the tight-junctions that associate apical poles of adjacent hepatocytes and seal the bile canaliculi formed

(48) Kukongviriyapan, V.; Stacey, N. H. *J. Cell. Physiol.* **1989**, *140*, 491–497.
(49) Ihrke, G.; Neufeld, E. B.; Meads, T.; Shanks, M. R.; Cassio, D.; Laurent, M.; Schroer, T. A.; Pagano, R. E.; Hubbard, A. L. *J. Cell. Biol.* **1993**, *123*, 1761–1775. Shanks, M. R.; Cassio, D.; Lecoq, O.; Hubbard, A. L. *J. Cell Sci.* **1994**, *107*, 813–825. Decaens, C.; Durand, M.; Grosse, B.; Cassio, D. *Biol. Cell* **2008**, *100*, 387–398.
(50) Roelofsen, H.; Wolters, H.; Van Luyn, M. J.; Miura, N.; Kuipers, F.; Vonk, R. J. *Gastroenterology* **2000**, *119*, 782–793.
(51) Guo, Y.; Nyasae, L.; Braiterman, L. T.; Hubbard, A. L. *Am. J. Physiol. Gastrointest. Liver Physiol.* **2005**, *289*, G904–G916.
(52) Collins, J. C.; Paietta, E.; Green, R.; Morell, A. G.; Stockert, R. J. *J. Biol. Chem.* **1988**, *263*, 11280–11283.

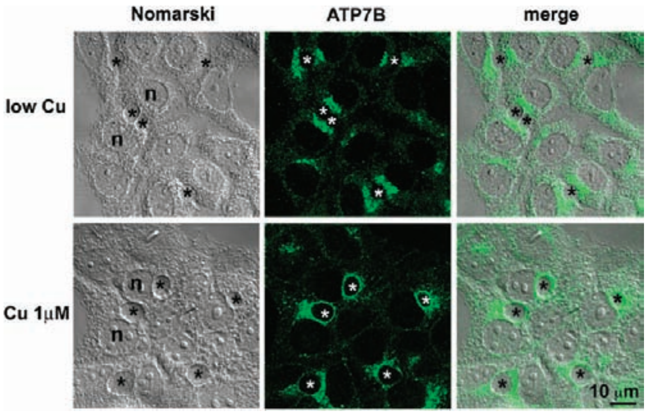

Figure 6. ATP7B localization in WIF-B9 cells—effect of copper concentration. ATP7B localization was detected by indirect immunofluorescence and imaged by confocal microscopy. WIF-B9 cells were kept in the basal culture medium (upper panel) or supplemented with 1 μM copper (lower panel) for 2 h. In each panel are presented from left to right, the Nomarski image, one confocal section taken in the middle of the cell layer, and the merge image. Bile canaliculi were indicated by asterisks; n: nucleus.

between cells.[53] ZO-1 was confined as dots or lines closing the bile canaliculi. In the control experiment (Figure 7A), most of the fluorescence signal localizing ATP7B was encircling bile canaliculi, as expected in high-Cu condition (Figure 6, lower panel). The diffusion around the canaliculi can be attributed to ATP7B molecules that were not yet at the canalicular membrane. In the presence of 10 μM **P**^{3} (Figure 7B), the distribution of ATP7B was different and became asymmetrical. ATP7B was no more present as continuous crowns around the bile canaliculi closed by ZO-1, but was now localized in a larger compartment reminiscent of the trans-Golgi network, situated near the nucleus, as in cells cultured in low Cu concentration (Figure 6, upper panel). To evaluate a possible role of the glycopeptide that would be independent of its affinity for copper, the experiment in high-Cu was repeated with **P^3-Ala,** a low affinity glycopeptide similar to **P**^{3} except for substituting alanines for the two cysteines (see SI Scheme S1). In this experiment, ATP7B localization (Figure 7C) was the same as that obtained without any glycopeptide (Figure 7A), indicating that the glycopeptide does not interfere with ATP7B trafficking. Therefore, these experiments provide evidence that the effect of **P**^{3} (Figure 7B) is due to its two cysteine residues which provide the high affinity for Cu(I).

To summarize, ATP7B intracellular localization indicates the disappearance of excess intracellular copper in the presence of **P^3**, thereby demonstrating its ability to lower intracellular copper. As we demonstrated that **P**^{3} is able to efficiently chelate Cu(I) in vitro in presence of GSH (Figure 4), these cell studies suggest that **P**^{3} acts as an intracellular copper chelator.

3. Conclusions

In the present work, we designed a molecule able to both complex intracellular copper, namely Cu(I), and target hepatocytes, combining a chelating unit with a carbohydrate recognition element within the same structure. A cyclodecapeptide scaffold displaying a controlled conformation with two independent faces was chosen to introduce the chelating and the recognition units. One face displays a cluster of carbohydrates to ensure an efficient recognition of ASGP-R, which are expressed on the surface of hepatocytes. The second face is devoted to metal ion complexation and a peptide sequence with two cysteines was selected to design the Cu(I) chelating unit. Indeed, cysteine-based peptides or pseudopeptides, inspired from some natural Cu(I) binding proteins appeared to be efficient Cu(I) complexing molecules. Another challenge was to obtain a chelator that would be activated by its entry inside the cells, in other words that would not be spoiled before reaching its final destination. To achieve this, the two thiol functions were oxidized in a disulfide bridge to afford the glycopeptide **P**^{3}, which is stable in the presence of oxygen and most importantly which is not an efficient chelator before entering the hepatic cells.

We demonstrated that the cyclodecapeptide scaffold bearing two cysteine side-chains on the same face are efficient binders of soft ions Cu(I) and Hg(II) with a high selectivity with respect to Zn(II). As expected **P**^{3} bearing hidden thiol functions oxidized in a disulfide bridge, is not a copper chelating agent, whereas once reduced by glutathione mimicking the intracellular reducing environment, **P**^{3} becomes an efficient Cu(I) chelator. The uptake of a fluorescent analogue of **P**^{3} by various hepatic cell lines proved the efficiency of the targeting unit. WIF-B9 cells which reconstitute polarized epithelia have offered a sensitive test to prove the intracellular copper lowering efficiency of **P**^{3} by monitoring the trafficking of the copper ATPase ATP7B. The glycocyclopeptide **P**^{3} can thus be considered as a prodrug activated in the reductive medium of the targeted cells to chelate excess Cu(I).

The redox properties of copper make it a toxic element for the cell when its homeostasis is disturbed. Therefore, the development of intracellular copper chelators such as **P**^{3} is of major interest to fight intracellular copper accumulation for patients suffering from Wilson's disease. The selectivity of **P**^{3} for Cu(I) with respect to Zn(II) is an important achievement as it allows to bind Cu(I) without perturbing Zn(II) homeostasis. Provided that a specific targeting unit can be defined, this strategy can be extended to many other cell types. In addition, since **P**^{3} has a high affinity for the toxic ion Hg(II), it could also be used as a mercury chelator.

4. Experimental Section

4.1. Peptide Synthesis. 4.1.1. Abbreviations. Ac_2O, acetic anhydride; DMF, *N*,*N*-dimethylformamide; DIEA, *N*,*N*-diisopropylethylamine; DTT, dithiothreitol; Et_2O, diethylether; Fmoc, 9-fluorenylmethyloxycarbonyl; PyBOP, (benzotriazole-1-yloxy)tris(pyrrolidino)phosphonium hexafluorophosphate; TFA, trifluoroacetic acid; TIS, triisopropylsilane; TRITC, tetramethylrhodamine isocyanate.

4.1.2. General Details. All chemical reagents and solvents were purchased from Aldrich or Acros and used without further purification. Protected amino acids were obtained from Advanced ChemTech, Bachem Biochimie, and France Biochem. 2-Chlorotrityl Chloride Resin and PyBOP were purchased from France Biochem. Mass spectra were acquired with an Esquire 3000 Bruker or with a LXQ type THERMO SCIENTIFIC spectrometer both equipped with a electrospray ionization (ESI) source or with a MALDI-TOF mass spectrometer BRUKER. The building blocks Fmoc-Lys[BocSer(tBu)]−OH and O-α-D-galactopyranosyl oxyamine (αGalNAcONH$_2$, **6**) were synthezised as previously described.[27,42] The low affinity glycopeptides **P^3-Ala** was synthesized as previously described.[25]

4.1.3. P^1 and P^2 Synthesis. The linear precursors with protected side-chains HArg(Pbf)-Cys(Trt)-Ser(*t*Bu)-Pro-Gly-Ser(*t*Bu)Cys(Trt)-Trp(Boc)Pro-Gly-OH and H-Trp(Boc)-Cys(Trt)-Glu(*t*Bu)-Pro-Gly-Glu(*t*Bu)-Cys(Trt)-Asp(*t*Bu)-Pro-Gly-OH were assembled manually by solid-phase peptide synthesis on 2-Chlorotrityl Chloride Resin (substitution 0.5 mmol/g, 500 mg) using Fmoc chemistry. Couplings were performed with *N*-α-Fmoc-protected amino acids (2 equiv), PyBOP (2 equiv), and DIEA (6 equiv) in DMF for 30 min. After each coupling, the resin was treated with DMF/pyridine/Ac_2O ($v/v/v$ = 7/2/1) to acetylate unreacted amino groups (2 × 5 min). Fmoc deprotection

(53) Decaens, C.; Rodriguez, P.; Bouchaud, C.; Cassio, D. *J. Cell Sci.* **1996**, *109*, 1623–1635.

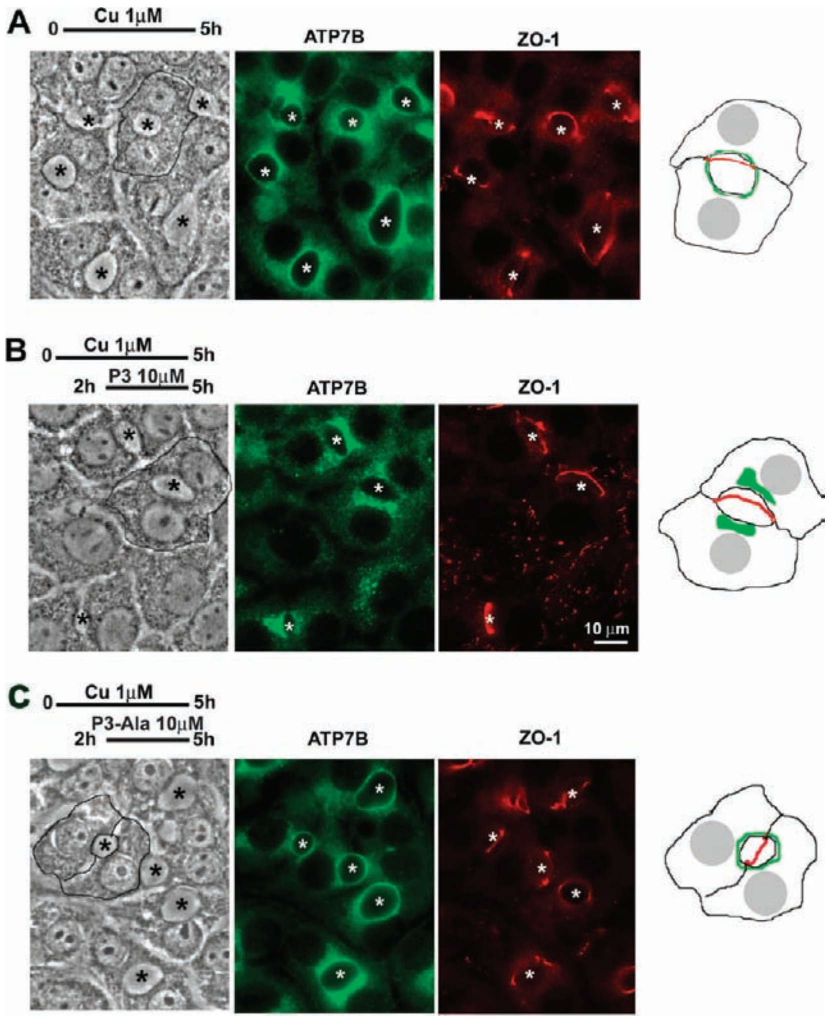

Figure 7. ATP7B localization in WIF-B9 cells—effect of $\mathbf{P}^3$. ATP7B and ZO-1 were localized by indirect immunofluorescence. WIF-B9 cells were kept in the presence of 1 μM Cu for 5 h (A,B,C) and 10 μM $\mathbf{P}^3$ (B) or $\mathbf{P}^3$**-Ala** (C) was added after 2 h and for a 3 h-period. The phase contrast images (left panels) allow direct visualization of the bile canaliculi indicated by asterisks. The localization of ZO-1 allows the visualization of tight junctions sealing bile canaliculi and gives a better view of the geometry of these structures. ATP7B is differently distributed in B, compared to A and C, as schematized in the right panels showing one doublet of WIF-B9 cells forming one bile canaliculus (the doublet schematized is underlined by a thin black line on the corresponding phase contrast image).

was achieved with DMF/piperidine ($v/v = 4/1$) (3×5 min). The yield of each peptide coupling was monitored by UV−vis spectroscopy (ε_{300}= 7800 L mol^{-1} cm^{-1} for the piperidine adduct dibenzofulvene). The peptide was cleaved from the resin by treatment with 15 mL CH_2Cl_2/TFA ($v/v = 99/1$) (2×3 min). The cleavage was performed very quickly, and the solution was flushed into 15 mL of Methanol/Pyridine solution ($v/v = 8/2$). After concentration, the residue was precipitated several times in cold Et_2O to obtain a white powder. The linear precursor was then reacted in CH_2Cl_2 (0.5 mM) with PyBOP (3 equiv) and DIEA (4 equiv). The cyclic peptide formation was followed by analytical HPLC and the reaction was completed after 10 min. CH_2Cl_2 was then evaporated. The oily residue was precipitated with CH_2Cl_2/Et_2O to yield the cyclic peptide as a powder. The side-chain protections were removed by treatment with a solution of 1.4 g DTT in TFA/TIS/H_2O/ ($v/v/v/v = 95/2.5/2.5$) (peptide concentration = 10 mM). After stirring for 2 h, the solution was evaporated under reduced pressure to yield yellow oil which was precipitated several times with cold Et_2O. The solid residue was dissolved in water/acetonitrile, filtered on PTFE 0.45 μm and purified by preparative RP-HPLC (Merck Purospher, 250 × 40 mm, 10 μm C18 particles, solvent A = H_2O/TFA ($v/v = 99.925/0.075$), solvent B = CH_3CN/H_2O/TFA ($v/v/v = 90/10/0.1$), gradient 5 to 45% of B in 30 min, flow rate 75 mL/min) to yield $\mathbf{P}^1$ as a white powder (52 mg, 19% overall yield), or $\mathbf{P}^2$ as a white powder (144 mg, 53% overall yield). Analytical RP-HPLC were performed using analytical column (Merck Purospher-STAR end-capped, 4.6 × 250 mm, 5 μm C18 particules) at 1 mL/min with UV monitoring at 214 nm. $\mathbf{P}^1$**:** Analytical HPLC Purity: 96%, Rt = 15.7 min (gradient 5 to 60% of B in 30 min). MALDI-TOF mass spectrometry: calculated for $C_{43}H_{62}N_{14}O_{12}S_2$, $[M+H^+]^+$ = 1031.41, exp = $[M+H^+]^+$ =1031.45. $\mathbf{P}^2$**:** Analytical HPLC Purity: 98%, Rt = 23.6 min (gradient 5 to 45% of B in 30 min). MALDI-TOF mass spectrometry: calculated for $C_{45}H_{59}N_{11}O_{16}S_2$, $[M+H^+]^+$ = 1074.36, exp = $[M+H^+]^+$ 1074.65.

4.1.4. $\mathbf{P}^3$ and $\mathbf{P}^3$-TRITC Synthesis. Analytical and preparative RP-HPLC analyses were performed using a Waters system, equipped with a UV detector (λ = 214 and 250 nm). HPLC analyses were performed on a Macherey-Nagel Nucleosil 120 Å 3 mm C18 particles (30 × 4.6 mm) using a gradient from solvent A (water/TFA ($v/v = 99.9/0.1$)) to solvent B (acetonitrile/water/TFA ($v/v/v = 90/10/0.1$)) at a flow rate of 1.3 mL/min. RP-HPLC was performed on a Delta-Pack 100 Å 15 mm C18 particles (200 × 2.5 mm) using the same gradient at a flow rate of 22 mL/min.

Synthesis of 4. The linear precursor with protected side-chains **1** was assembled manually by solid-phase peptide synthesis on 2-Chlorotrityl Chloride Resin (substitution 0.4 mmol/g, 0.507 g, 0.202 mmol) using Fmoc chemistry.[54] The resin was swollen with CH_2Cl_2 (10 mL, 1 × 10 min) and DMF (10 mL, 1 × 10 min). Couplings were performed with N-α-Fmoc-protected amino acids

(54) Sheppard, R. *J. Pept. Sci.* **2003**, *9*, 545–552.

or Fmoc-Lys[Boc-Ser(*t*Bu)]−OH (2.5 equiv, 0.5 mmol), PyBOP (2.5 equiv, 0.5 mmol) and DIEA (pH ≈ 8−9) in DMF (10 mL) for 30 min. After washing with DMF (10 mL, 4 × 1 min) and CH_2Cl_2 (10 mL, 2 × 1 min), the completeness of the coupling reaction was controlled by Kaiser or TNBS tests. *N*-α-Fmoc protecting groups were removed by treatment with a DMF/piperidine solution (v/v = 4/1, 10 mL, 3 × 10 min). After washing with DMF (10 mL, 6 × 1 min), the completeness of deprotection was verified by the UV absorption of piperidine washings at 299 nm. After the last coupling reaction, on-resin **1** was obtained (0.13 mmol, yield = 64%). The resin (0.13 mmol) was swollen with CH_2Cl_2 (10 mL, 1 × 10 min) and DMF (10 mL, 1 × 10 min). Iodine (0.660 g, 2.60 mmol) and DMF (10 mL) were added. The reaction mixture was stirred at room temperature during 1.5 h. After filtration, the resin was washed with DMF (10 mL, 6 × 5 min), DMF/Water v/v = 1/1 (10 mL, 2 × 5 min), DMF (10 mL, 1 × 5 min) and CH_2Cl_2 (10 mL, 3 × 5 min). The peptide was then cleaved from the resin by treatment with CH_2Cl_2/TFA (v/v = 99/1, 10 mL, 10 × 2 min). The filtrate was recovered and DIEA (1 mL) was added to avoid deprotection during the evaporation. After concentration, the residue was precipitated in Et_2O. The linear precursor was then reacted in DMF (∼0.5 mM) with PyBOP (0.074 g, 0.14 mmol) and DIEA (0.08 mL, 0.39 mmol) for 2 h. DMF was evaporated under reduced pressure. The oily residue was precipitated with CH_2Cl_2/Et_2O to yield the cyclic peptide **3** as a powder. Removal of side-chain protecting groups was performed in TFA/H_2O/ (v/v = 90/10, 20 mL). After stirring for 2 h, the solution was evaporated to yield a yellow oil which was precipitated with Et_2O to obtain the deprotected peptide **4** as a white solid (0.097 g, 0.067 mmol, 33%). Analytical HPLC Purity: 83%, *Rt* = 6.13 min (Linear gradient: 95/5 to 60/40 A/B in 15 min). ESI-MS calculated for $C_{60}H_{105}N_{19}O_{18}S_2$, $[M+H^+]^+ = 1444.74$, exp: $[M+H^+]^+ = 1444.58$, $[M+2H^+]^{2+} = 722.92$, $[M+3H^+]^{3+} = 482.33$.

Synthesis of 5. To a solution of compound **4** (0.064 g, 0.044 mmol) in water (8 mL), sodium periodate (0.380 g, 1.77 mmol) was added. After 15 min, the reaction mixture was injected in RP-HPLC (*Rt* = 14 min, linear gradient: 95/5 to 60/40 A/B in 15 min), to yield **5** as a white powder (0.009 g, 0.0068 mmol,15%) after lyophilization. ESI-MS calculated for $C_{56}H_{85}N_{15}O_{18}S_2$, $[M+H^+]^+ = 1320.57$, exp: $[M+H^+]^+ = 1320.5$.

Synthesis of P^3. To a solution of compound **5** (0.025 g, 0.019 mmol**)** in AcOH/water (4 mL, v/v = 1/9), O-α-D-galactopyranosyl oxyamine (**6**) was added (0.045 g, 0.192 mmol). The reaction mixture was stirred at room temperature during 1 h. Then, the mixture was injected in RP-HPLC (*Rt* = 14−16 min, linear gradient: 95/5 to 60/40 A/B in 15 min) to yield $\mathbf{P}^3$ as a white powder (0.021 g, 0.0096 mmol, 50%) after lyophilization. Analytical HPLC Purity: 95%, *Rt* = 9.25 min (linear gradient: 100% water to 50/50 water/acetonitrile in 16 min). ESI-MS: calculated for $C_{88}H_{141}N_{23}O_{38}S_2$, $[M+H^+]^+ = 2192.92$, exp: $[M+H^+]^+ = 2193.5$.

Synthesis of P^3-TRITC. TRITC (0.003 g, 0.0067 mmol) and a few drops of DIEA (pH ≈ 8−9) were added to a solution of compound $\mathbf{P}^3$ (0.012 g, 0.0055 mmol) in DMF (2 mL). The reaction mixture was stirred at room temperature during 2 h and injected in RP-HPLC (*Rt* = 19 min, linear gradient: 95/5 to 60/40 A:B in 15 min) to yield $\mathbf{P}^3$**-TRITC** as a pink powder (0.0012 g, 0.00046 mmol, 8%) after lyophilization. Analytical HPLC Purity: 90%, *Rt* = 14.4 min (linear gradient: 100% water to 50/50 water/acetonitrile in 16 min). ESI-MS: calculated for $C_{113}H_{163}N_{26}O_{41}S_3^+$, $[M]^+ = 2637.1$, exp: $[M]^+ = 2636.6$, $[M^+ + H^+]^{2+} = 1318.9$.

Peptides $\mathbf{P}^1$, $\mathbf{P}^2$, and **4** were characterized by ^1H NMR and the corresponding chemical shift tables are Tables S1, S2, and S3, respectively, of the SI. The NMR experiments were recorded on a 500 MHz Bruker Avance spectrometer equipped with a BBI probe with triple axis gradient field. ^1H NMR spectra were recorded with 12 ppm windows and 32 k data points in the time domain. 2D ^1H NMR spectra were recorded at 298 K in H_2O/D_2O (v/v = 9/1) using Watergate[55] or presaturation solvent suppression. 2D spectra were acquired in phase-sensitive mode with TPPI for quadrature detection in the indirect dimension, using 2048 × 256 (TOCSY) or 2048 × 512 (ROESY) matrices over a 6000 Hz spectral width. TOCSY experiments were performed using a MLEV-17 spin-lock sequence with a mixing time of 70 ms. Off-resonance ROESY[56] experiments were recorded with a mixing time of 300 ms (4050 Hz spin-lock). H−H distances were obtained by integrating the cross peaks in the Roesy spectrum and taking Gly Hα1/Hα2 and well-resolved X Hβ1/Hβ2 (1.80 Å) cross correlations as references for distance calibration.

4.2. Physico-Chemical Studies. 4.2.1. Solution Preparation. Since the cysteine residues are susceptible to air oxidation, all the solutions were prepared in a glovebox under argon atmosphere. Fresh solutions of the ligand were prepared before each experiment in the appropriate buffer (20 mM) and acetonitrile (v/v = 9/1) using deoxygenated Milli-Q water (Millipore). The final concentration of the ligand solution was determined by measuring the cysteine free thiol concentration following the Ellman's procedure.[57] This procedure uses 5,5′-Dithiobis-2-nitrobenzoic acid (DTNB) as an indicator: each free thiol group present in the peptide yields 1 equiv of TNB^{2-} ($\epsilon^{412\ nm}$ (TNB^{2-}) = 14 150 $M^{-1}\cdot cm^{-1}$).

Cu(I) solutions were prepared by dissolving the appropriate amount of $Cu(CH_3CN)_4PF_6$ in deoxygenated acetonitrile. The final concentration was determined by adding an excess of sodium bathocuproine disulfonate (Na_2BCS) and measuring the absorbance of $Cu(BCS)_2^{3-}$ (λ_{max} = 483 nm, ϵ = 13 300 $M^{-1}cm^{-1}$). The other metal solutions were prepared from the corresponding salt ($CdCl_2$, $HgCl_2$, $PbCl_2$ or $ZnCl_2$) in deoxygenated water or in the appropriate buffer and titrated by 5 mM volumetric EDTA (Fisher Chemicals) in presence of a colorimetric indicator.

4.2.2. UV Titrations. The UV−visible spectra were recorded with a Varian Cary50 spectrophotometer equipped with optical fibers connected to an external cell holder in the glovebox. Two milliliters of the ligand solution (∼50 μM) were transferred in a UV cell (1 cm path) and aliquots corresponding to 0.1 equiv of the metal solution were then added. The buffer was phosphate (20 mM, pH 7.4) for all of the titrations except for Pb(II), for which Bis-Tris (20 mM, pH 7) was used to prevent Pb(II) hydrolysis and the precipitation of $Pb(OH)_2$.[40]

4.2.3. CD Titrations. The circular dichroism spectra were acquired with an Applied Photophysics Chirascan spectrometer. 2.5 mL of the ligand solution (∼50 μM in phosphate buffer, 20 mM, pH 7.4) were transferred in a UV cell (1 cm path) and aliquots corresponding to 0.25 equiv of the Cu(I) solution in acetonitrile were then added. CD spectra are reported in molar ellipticity ([Θ] in units of degcm^{2}dmol^{-1}). $[\Theta] = \theta_{obs}/(10lc)$, where θ_{obs} is the observed ellipticity in millidegrees, *l* the optical path length of the cell in centimeters, *c* the peptide concentration in moles per liter.

4.2.4. ESI-MS Titrations. Mass spectra were acquired on a LXQ-linear ion trap (THERMO Scientific, San Jose, USA) equipped with an electrospray source. Electrospray full scan spectra in the range *m/z* = 150 −2000 amu were obtained by infusion through a fused silica tubing at 2−10 μL/min. The solutions were analyzed in the negative and positive modes. The LXQ calibration (*m/z* = 50−2000) was achieved according to the standard calibration procedure from the manufacturer (mixture of caffeine, MRFA and Ultramark 1621). The temperature of the heated capillary for the LXQ was set to 180−200 °C, the ion-spray voltage was in the range 2−4 kV and the injection time was 10−100 ms. The ligand solution (100 μM) was prepared in ammonium acetate buffer (20 mM, pH 7)/acetonitrile (v/v = 9/1) and aliquots of the metal solution were then added.

(55) Piotto, M.; Saudek, V.; Sklenar, V. *J. Biomol. NMR* **1992**, *2*, 661–665.
(56) Desvaux, H.; Berthault, P.; Birlirakis, N.; Goldman, M.; Piotto, M. *J. Magn. Reson. A* **1995**, *113*, 47–52.
(57) Riddles, P. W.; Blakeley, R. L.; Zerner, B. *Methods Enzymol.* **1983**, *91*, 49–60.

4.2.5. Apparent Affinity Constant Determination. Cu(I). The apparent stability constants at pH 7.4 of the two Cu(I) complexes, were measured by UV−visible titrations in presence of bathocuproine disulfonate (BCS) as a competitor. The complexes were prepared by adding 0.8−0.9 equiv of the Cu(I) solution in acetonitrile to the ligand solution in Phosphate buffer (20 mM pH 7.4)/acetonitrile ($v/v = 9/1$). The mixture was stirred for 10 min to ensure the formation of the complex, which was checked by recording the absorption at 262 nm. Aliquots of a BCS solution (10 mM in phosphate buffer, 20 mM, pH 7.4) were then added to the Cu(I) complexes. The UV/vis spectra were recorded and show the formation of the orange $Cu(BCS)_2$ complex. The stability of the absorbance was controlled before the addition of any other aliquots. The data were analyzed according to the formation of a Cu**P** complex, with the characteristics of the complex $Cu(BCS)_2$ fixed to the values: $\epsilon = 13\,300$ mol^{-1}Lcm^{-1} at 483 nm and $\log\beta_{12} = 19.8$.

Pb(II). The apparent stability constant at pH 7 of the Pb(II) complex was measured by fitting the titrations of $\mathbf{P}^i$ by Pb(II) in the buffer Bis-Tris (20 mM, pH 7). The affinity of Bis-Tris for Pb(II) was included in the fit ($\log\beta_{11} = 4.32$).[58] Two absorbing species were detected with $\mathbf{P}^1$ (Pb$\mathbf{P}^1$ and Pb($\mathbf{P}^1$)$_2$), whereas only one absorbing species was detected with $\mathbf{P}^2$ (Pb$\mathbf{P}^2$).

Cd(II) and Zn(II). The apparent stability constants at pH 7 of the Cd(II) and Zn(II) complexes were measured by fitting the disappearance of the lead complex absorbance by addition of aliquots of these metal ions in Bis-Tris (20 mM, pH 7). During these back-titrations, aliquots of Cd(II) or Zn(II) solutions in Bis-Tris 20 mM were added to the UV cell containing the lead complex in Bis-Tris 20 mM pH 7, made of 1 ligand equiv and 3 Pb(II) equiv. The affinities of these metal ions for Bis-Tris are known and were included as parameters in the fit ($\log\beta_{11}$= 2.47 (Cd), 2.38 (Zn)).[58] The apparent stability constant of PbL was also included as a parameter in the fit of the back-titrations.

Hg(II). The back-titration of the Cu(I) complexes of $\mathbf{P}^1$and $\mathbf{P}^2$ with a Hg(II) solution shows the total disappearance of the S−Cu LMCT band for 1 equiv of added Hg(II). The data were simulated with more than 97% of Cu(I) displaced from the ligand at the end of the titration.

4.3. Cell Studies. 4.3.1. General Culture Conditions. HepG2 cells were grown in Dulbecco's modified Eagle's medium (DMEM) supplemented with 10% v/v fetal bovine serum (FBS), 20 mM L-glutamine, 10 mM sodium pyruvate, 100 μg/mL streptomycin and 100 U/mL penicillin. WIF-B9 cells were grown in Coon's modified F12 medium (Sigma) supplemented with HAT (10^{-5} M hypoxanthine, 4×10^{-8} M aminopterin, 1.6×10^{-4} M thymidine), 5% FBS (Invitrogen), 2 mM glutamine, and an antibiotic and antifungal solution containing 100 μg/mL streptomycin, 100 U/mL penicillin, and 0.25 μg/mL amphotericine B. Cells were cultured at 37 °C in a humidified atmosphere with 5% (HepG2) or 7% (WIF-B9) CO_2. They were plated at 2×10^4 cells/cm^2 on plastic tissue culture dishes (Falcon) or on round (16 mm in diameter) or square (22 ×22 mm) autoclaved glass coverslips (Esco) in 6, or 12-well plates and used 7−9 days later. The culture medium was renewed every 2 to 3 days.

4.3.2. Localization of ATP7B by Immunofluorescence. Cells on glass coverslips were rinsed three times in phosphate-buffered saline (PBS) and permeabilized with methanol for 4 min at −20 °C. They were then rehydrated in PBS and incubated at 37 °C for 45 min, either with a rabbit primary antibody anti-ATP7B (1/200 diluted), or with this ATP7B antibody and a rat monoclonal antibody anti-ZO1 (undiluted). After 3 rinses with PBS, the cells were incubated for 15 min at 37 °C with a goat antirabbit antibody conjugated with Alexa 488 (1/500; Molecular Probes) or with a mixture of this latter antibody and a goat antirat antibody conjugated with Alexa 566 (1/500; Molecular Probes). Cells were then washed three times in PBS and the coverslips were mounted on glass slides with a drop of mounting medium (Sigma) and sealed using nail polish. The cells were analyzed using a Zeiss fluorescence Axioskop microscope. Confocal analysis was performed with a Zeiss LSM 510 microscope and series of *xy* sections were taken in 0.3 μm steps. The rabbit primary antibody anti-ATP7B was from I. Sandoval (CIBEREHD, Madrid, Spain) and was directed against the NH_2-terminal 655 residues of human ATP7B.[59] The rat primary monoclonal antibody anti-ZO-1 was from B. Stevenson (University of Alberta, Edmonton, Canada).

4.3.3. Uptake of $\mathbf{P}^3$-TRITC. The uptake of $\mathbf{P}^3$-TRITC by HepG2 and WIF-B9 cells was explored using a concentration range of 2 to 0.2 μM. $\mathbf{P}^3$-TRITC was added in the medium and at regular intervals, cells on coverslips were rinsed twice with phosphate buffer saline (PBS), fixed with 4% formaldehyde for 20 min and viewed on Zeiss fluorescence microscopes (Axioskop or AxioVert 200M). The 2 μM concentration was also left for up to 4 days without damaging neither HepG2 nor WIF-B9 cells.

4.3.4. Trafficking of ATP7B. Trafficking of ATP7B has been shown before in various cell lines under extreme conditions, such as addition of 200 μM BCS or 20−200 μM copper in the culture medium.[51] Since we wanted to avoid the use of high concentrations of $\mathbf{P}^3$, we had to find conditions inducing ATP7B trafficking at lower concentrations of copper and within a few hours to avoid cellular responses involving protein synthesis. No ATP7B trafficking could be detected after 2 h in 0, 0.1, and 0.3 μM copper added to the medium. Trafficking was clear after 2 h in the presence of 1 μM copper. Starting from this observation, two concentrations of $\mathbf{P}^3$ were tested for their ability to reverse the trafficking of ATP7B. As shown in Figure 7, there was a clear-cut answer after 3 h in the presence of 10 μM $\mathbf{P}^3$, whereas 2 μM was not enough (data not shown). A control experiment with the low affinity glycopeptides **$\mathbf{P}^3$-Ala** 10 μM was performed to demonstrate that the ability of $\mathbf{P}^3$ to reverse the trafficking of ATP7B was due to the presence of the two cysteine residues.

Acknowledgment. We thank Michel Ferrand for very fruitful discussions at the beginning of this project. We are grateful to Ignacio Sandoval (CIBEREHD, Madrid, Spain) for his generous gift of a polyclonal antibody anti-ATP7B. We thank Valérie Nicolas (IFR 141, Plateforme d'Imagerie Cellulaire, Chatenay Malabry, France) for help with confocal analysis and Yves Chenavier for performing some of the titration experiments. We thank the "Université Joseph Fourier" (UJF-Grenoble), the "Centre National de la Recherche Scientifique" (CNRS), and the NanoBio program for the access to the facilities of the Synthesis platform. Financial support from the "Cluster de Recherche Chimie de la Région Rhône-Alpes" is duly acknowledged.

Supporting Information Available: Peptides $\mathbf{P}^1$, $\mathbf{P}^2$, and **4** 500 MHz ^{1}H NMR characterization, short proton−proton distances in the turn regions of $\mathbf{P}^1$ and $\mathbf{P}^2$, ESI-MS of divalent metal ion complexes of $\mathbf{P}^1$ and $\mathbf{P}^2$, UV titrations of $\mathbf{P}^1$ and $\mathbf{P}^2$ with divalent metal ions, formula of **$\mathbf{P}^3$-Ala**. This material is available free of charge via the Internet at http://pubs.acs.org.

JA106206Z

(58) Scheller, K. H.; Abel, T. H.; Polanyi, P. E.; Wenk, P. K.; Fischer, B. E.; Sigel, H. *Eur. J. Biochem.* **1980**, *107*, 455–466. Magyar, J. S.; Godwin, H. A. *Anal. Biochem.* **2003**, *320*, 39–54.

(59) Hernandez, S.; Tsuchiya, Y.; Garcia-Ruiz, J. P.; Lalioti, V.; Nielsen, S.; Cassio, D.; Sandoval, I. V. *Gastroenterology* **2008**, *134*, 1215–1223.